Res. Lett. Inf. Math. Sci., 2012, Vol. **16**, pp. 1–22
Available online at http://iims.massey.ac.nz/research/letters/

Leaf Area Index and Topographical Effects on Turbulent Diffusion in a Deciduous Forest

S. KIMURA[1], R. MCKIBBIN[2], J. OGAWA[3], T. KIWATA[3], N. KOMATSU[3], K. NAKAMURA[1]

[1] *Institute of Nature and Environmental Technology*
Kanazawa University, Kanazawa 920-1192, Japan

skimura@t.kanazawa-u.ac.jp

[2] *Institute of Information and Mathematical Sciences*
Massey University, Albany Campus,
Private Bag 102 904, North Shore Mail Centre
Auckland New Zealand 0745

R.McKibbin@massey.ac.nz

[3] *School of Mechanical Engineering*
Kanazawa University, Kanazawa 920-1192, Japan

Abstract In order to investigate turbulent diffusion in a deciduous forest canopy, wind velocity measurements were conducted from late autumn of 2009 to early spring of 2010, using an observation tower 20 m in height located in the campus of Kanazawa University. Four sonic anemometers mounted on the tower recorded the average wind velocities and temperatures, as well as their fluctuations, at four different heights simultaneously. Two different types of data sets were selected, in which the wind velocities, wind bearings and atmospheric stabilities were all similar, but the Leaf Area Indexes (LAI's) were different. Vertical profiles of average wind velocities were found to have an approximately exponential profile in each case. The characteristic length scales of turbulence were evaluated by both von Karman's method and the integral time scale deduced from the autocorrelation from time-series analyses. Both methods produced comparable values of eddy diffusivity for the cases with some foliage during late autumn, but some discrepancy in the upper canopy layer was observed when the trees did not have their leaves in early spring. It was also found that the eddy diffusivities generally take greater values at higher positions, where the wind speeds are large. Anisotropy of eddy diffusivities between the vertical and horizontal components was also observed, particularly in the cases when the canopy does not have leaves, when the horizontal eddy diffusivities are generally larger than the vertical ones. On the other hand, the anisotropy is less visible when the trees have some foliage during autumn. The effects of topography on the turbulent diffusion were also investigated, including evaluation of the non-zero time-averaged vertical wind velocities. The results show that the effects are marginal for both cases, and can be neglected as far as diffusion in the canopy is concerned.

Keywords: canopy flow, turbulence, eddy diffusivity, forest canopy, deciduous forest, micro-climate, complex terrain.

1 Introduction

Turbulent dispersion processes are largely responsible for defining the environmental conditions in our atmosphere. Air-flows near the Earth's surface, particularly in the surface layers, are affected by the surface roughness (which is associated with urban structures and plant canopies) as well as the terrain topography. Plant canopies are a common occurrence on the Earth's surface, and the turbulent diffusion processes there play an important role in controlling dispersion of pollens, seeds, smoke and fire sparks from forest fires, other airborne particles, as well as concentrations of water vapour, CO_2 and other gaseous substances within and above the canopies. The air-flows within the vegetation layer are responsible for a broad range of transport processes in connection with our atmospheric environment, in forest ecological and biological systems [e.g. see Kaimal & Finnigan (1994), Kantha & Clayson (2000), Langre (2008)]. In addition, the investigation of flows within plant canopies helps us to understand the mechanisms of other effects on our environment, for instance:

windshield, moderation of severe heat during summer time, protection against wind abrasion, trapping of atmospheric pollutants. However, our understanding about the transport mechanisms in tall plant canopies is still very limited due to the difficulty of conducting field measurements, and also by diverse conditions appearing in the canopy structures and surrounding topographies [e.g. see Finnigan (1979), Kondo & Akashi (1975), Raupach *et al*. (1996), Shaw *et al*. (1974)].

In general, the dispersion of airborne particles and gaseous substances is significantly affected by random fluid motions in atmosphere (turbulent eddies); this agitated air flow leads to significantly enhanced transport of momentum and scalar quantities (heat, water vapour, CO_2, etc). For plant canopy layers, many field measurements were reported up until the early 1990's. Some of the earliest work goes back to the description of *honami*, which refers to travelling waves over wheat and rice fields (Inoue, 1955). Since then, a large amount of literature has been produced on this subject. Reviews and summaries of the effect of plants on turbulent flows may be found in Raupach & Thom (1981) and Finnigan (2000).

During the late 1980's and in the 1990's a new research trend emerged, associated with the control of air quality in urban canopies [see, for example, Uno *et al*. (1988), Rotach (1993), Roth & Oke (1993) and Oikawa & Meng (1995)]. This shift in research emphasis took place naturally, because of the urgent need to understand the mechanisms of heat-island formation phenomena and dispersion processes of airborne pollutants in urban environments. Many relevant studies employed numerical techniques to analyse the formation of heat islands and the dispersion of airborne pollutants in urban canopies. One of the difficulties challenging them, however, is to evaluate the turbulent diffusivities of momentum, heat and species in a model system of convection-diffusion equations.

The turbulent diffusivity is also called the eddy diffusion coefficient, or mechanical dispersion coefficient, which we denote K in this paper. Values of K have been reported for both plant and urban canopies. However, as for plant canopies, the measurements were conducted mainly in maize, rice and wheat fields in the early days [e.g. Uchijima (1962)], and only a limited number of measurements of K and the related turbulent parameters in the forest with tall trees were reported by such authors as Allen (1968), Amiro (1990), Gao *et al*. (1989). One of their important findings is a length scale, of order 10 m, in the forest canopy turbulence. However, on gusty and windy days the eddy length scale computed from the spectral powers of wind velocities becomes as large as 100 m [e.g. Allen (1968)]. Efforts to understand the turbulent nature in the plant canopy are still on-going, and can be found in more recent works by Marcolla *et al*. (2003), Poggi *et al*. (2004), Launiainen *et al*. (2007), Schleppi *et al*. (2007) and Yi (2008), which cover both theoretical aspects and experimental measurements.

Despite the large amount of work conducted up until now, it is interesting to note that little explicit data of turbulent diffusivity for tall forest canopies is available, although one may make estimations from the reported turbulent intensities and the length scales. Turbulent diffusivities are very important in solving advection-diffusion equations in the canopies for the purpose of predicting the moisture and temperature changes, as well as the dispersion of pollens and seeds in forests, with the aim of understanding ecological and biological systems, especially when analytical forms of the solutions to quantitative models are sought.

In connection with the mathematical development for analytical solutions of the advection-diffusion equation over the last few years, efforts have been made to construct simplified models for the aerial concentrations and, in particular, the subsequent deposit on the ground, of particles released into the atmosphere by dust- or sand-storms, volcanic eruptions, etc. Such releases take place at various elevations, and are composed of particles with a range of sizes; the wind's speed and turbulence profile may also vary with altitude. The aerosols may change their settling speed as they travel, due to agglomeration, evaporation or condensation, or adsorption. The inverse problem of trying to find the source from a given deposit was investigated by McKibbin (2003). As with many inverse problems, it may be ill-conditioned. The forward model for aerosol dispersion was investigated by McKibbin *et al*. (2005), Lim *et al*. (2008, 2008), McKibbin (2006, 2008, 2010) and Harper *et al*. (2010). The trapping of aerosols on foliage was included in models described in McKibbin (2006, 2008) and Harper *et al*. (2010); the latter paper also included the effects of evaporation from the particles' surface, thereby reducing the settling speed of the aerosols as they travelled.

Although the formulation of the problem is straightforward in many aspects, the estimation of the dispersion parameters in these simplified models has been problematical. So far, the turbulent diffusion coefficients in the relevant terms in the model equations have been estimated by considering the process for the particles as mechanical dispersion. The length scale of the turbulence in the atmosphere has been represented by an average value l, and, using a mechanical dispersion model, the dispersion coefficients K have been estimated using a standard formula $K = Ul$, where U is the wind speed. With an additional assumption that is

commonly used in volcanological models, i.e. that the vertical dispersion may be neglected, analytical formulae have been derived for deposit distributions from releases into a wind that varies with elevation, and which allow for change in settling speed as well as trapping of aerosols by vegetation during the last stages of descent (McKibbin, 2008). However, the problem of estimating suitable turbulence length scales within forest canopies that change with the seasons has remained. The analysis of the data collected in forest, therefore, may help to provide such estimates, and the models of aerosol passage through such canopies will benefit.

Aiming at providing such essential information, we have conducted measurements of the eddy diffusivities and other turbulent properties in a deciduous forest canopy, which is situated in relatively complex terrains, called *satoyama*. *Satoyama* is a hilly region covered with various trees, often situated near farming villages, and commonly observed throughout the countryside in Japan. The measurements took place from late autumn of 2009 to early spring of the next year. The present study is two-fold. First, the focus is on the effects of the LAI (Leaf Area Index) on the turbulent diffusivities. In order to highlight the effect, two typical measurement data sets are compared, while keeping the other conditions as close as possible. Since the measurements were performed in a forest that covers relatively complex terrain, the second interest is to address the effects of the surrounding topography on the wind and turbulence properties in the forest canopy sub-layer. It is noted that Finnigan (2000) expressed "canopies on hills" as one of the important future research problems.

2 Observation Site and Measurements

2.1 Observation Site

The field measurements were conducted in the campus of Kanazawa University from late autumn of 2009 to early spring of 2010. As shown in Figure 1, the observation site, a 20 m tall tower, is located on one of the minor ridges branching out from the major hill of about 130 m in altitude (E 136˚42'14", N 36˚32'47"). The major ridge is about 500 m in length and 50 m in width, stretching towards the north-west. The minor ridges, on one of which the observation tower is located, stretch toward the north and descend in that direction with a mean slope angle $\alpha = 16^{\circ}$. The two sides of this ridge, facing west and east respectively, form relatively steep slopes at about 30˚. There are several similar branching ridges oriented in parallel. They are all thickly covered with many tall deciduous trees, such as oak (*Quercus serrata*) and Japanese chestnut oak trees (*Quercus acutissima*), with occasional bamboo communities intruding into the oak community. The observation tower is surrounded predominantly by oak trees, many of which are as tall as the tower. The number of 20 m tall trees is 21 stems in the 400 m^2 area around the tower; the count of 10 m tall trees is 16 stems in the same area. The average height of the tallest trees is about 23 m.

2.2 Instrumentation

Wind velocities and temperatures were measured using four 3-D sonic anemometer-thermometers. Two of them are KAIJO, SAT550 (velocity resolution: 0.01 m/s; temperature resolution: 0.01 K) and the other two are YOUNG, model 81000 (velocity resolution: 0.01 m/s; temperature resolution: 0.01 K). The sonic anemometers were calibrated in a Kanazawa University wind tunnel. All data were collected by a data acquisition system (Keyence Co., NR-500) at a sampling rate of 10 Hz. Whenever mean values were needed, the acquired data were averaged over ten minutes. Data acquired over two-hour periods are the subject for analysis in the present study.

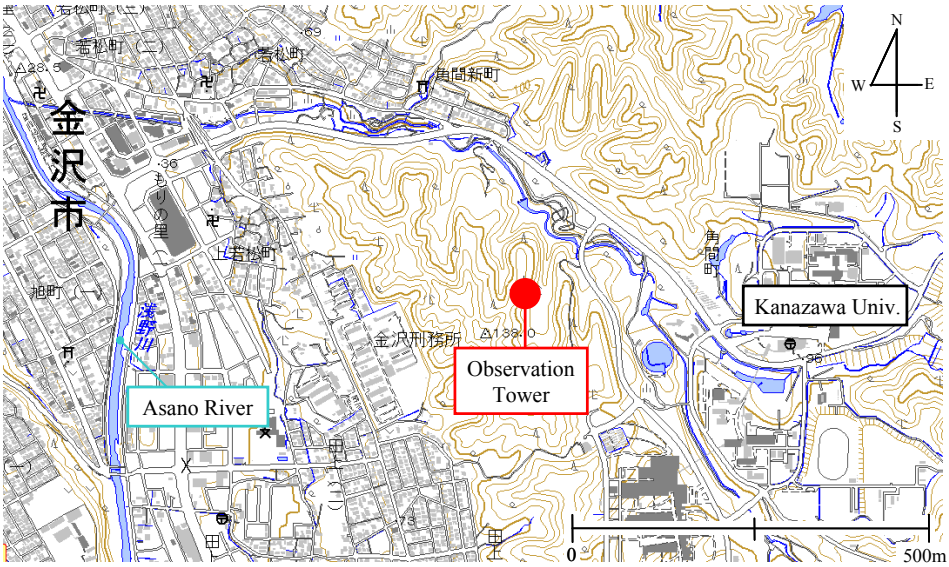

Figure 1. A map showing the location of the observation tower (a red circle in the center) and the surrounding topography (taken from the Kanazawa area 1/25000 Geographical map, Geographical Information Authority of Japan). The area is bounded in the west by commercial and residential areas, where the Asano river runs in a north to north-west direction, and in the east is bounded by buildings of Kanazawa university. Further eastwards, the area is covered by forest; the elevation increases gradually over a distance of 10 km until it reaches a ridge with an elevation of approximately 900 m.

2.3 Measurement Heights

Figure 2 shows a schematic of the field measurement system. The highest measurement position is 22.5 m above the ground. As shown in Figures 3(a) and 3(b), the observation tower is surrounded by dense oak trees whose average heights are about 23 m. Three anemometers are mounted on arms 1 m long stretched outwards from the tower, at vertical positions of 7.7 m, 14.6 m and 19.2 m respectively on the west side of the observation tower. The fourth probe is set at a vertical distance of 2.5 m from the top of the tower and about 1 m off the vertical line through the other three anemometers.

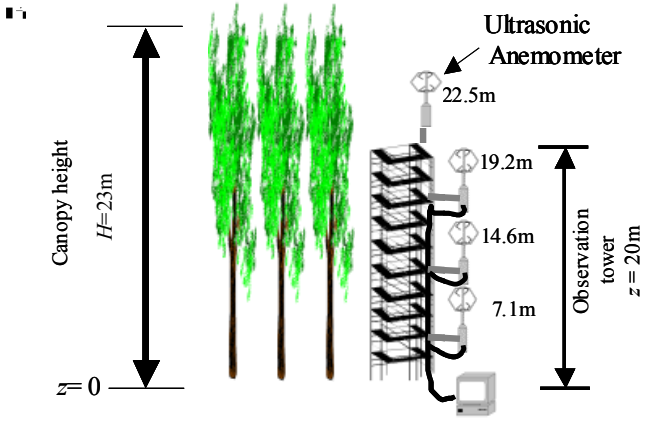

Figure 2. Schematic diagram of observation tower. It is surrounded by tall deciduous trees, whose heights are about 23 m on average. The tower was originally built to study insect migration, and its relation with the micro-climate in the forest.

2.4 Atmospheric Conditions

The data reported in this study are classified into two categories. In the first category, the data were acquired in the period between 11 and 23 March, 2010. Figure 3(a) shows a view of the tower during this period of time. As can be seen in the photograph, there were no leaves on the tree branches. The weather was fine or cloudy, and the mean horizontal wind velocity U_H at the canopy top was about 2 m s^{-1}. In the second category, the data were acquired in the period between 14 and 27 November, 2010, when the trees had some leaves as seen in Figure 3(b), and the LAI (Leaf Area Index) during this period was 1.49. The spatially-averaged LAD (Leaf Area Density) was about 0.25 m^2 m^{-3}, which is about 50% of the full foliage in summer time. The weather was also fine or cloudy, and the wind velocity U_H was again about 2 m s^{-1}.

(a)

(b)

Figure 3. Photographs of the observation tower: (a) in March 2010; (b) in November 2009.

Table 1 shows the various atmospheric conditions, such as atmospheric stabilities, wind velocities and wind bearings, on the respective days. The atmospheric conditions are quite similar in those data sets, except for the LAI. Therefore, the major difference between the two categories appears only in the LAI. However, it may be seen that the atmosphere is less stable in the 11 March data; this is probably due to the remains from clear unstable conditions that occurred in the morning of the same day. All of the data in Table 1 were measured at z

= 22.5 m, the highest measurement position (where z indicates the vertical coordinate measured from the ground); T_H is the mean temperature at the same height. The quantity L is the Monin-Obukhov stability length defined by $L = -u_*^3 T_0 / \kappa g(-w'T')$, where w' and T' are the fluctuations from the mean of the vertical wind velocity and temperature respectively, κ is the von Karman constant, T_0 is the potential temperature, g is the acceleration due to gravity, and u_* is the friction velocity defined by $u_* = \sqrt{-\overline{u'w'}}$. The ratio of z to L is a parameter that measures atmospheric stability at the height z. Although some variations in H/L are seen in Table 1, the absolute values are not very great, and less than 0.05. All of the values of H/L in Table 1 indicate that buoyancy forces are not significant in the cases studied.

Figure 4 shows the probability density of wind speed observed over the period from mid-November 2009, to the end of March 2010. Most of the observations during the period fall between 1.5 m s^{-1} and 3.5 m s^{-1}, in which the velocity of 2 m s^{-1} (representing the mean in the range 1.75 m s^{-1} ≤ U ≤ 2.25 m s^{-1}) has the highest density. A westerly wind was the most frequent occurrence during the same period. So a velocity of 2 m s^{-1} and a westerly wind were chosen as the typical weather conditions.

Table 1. Summary of wind and atmospheric conditions. The wind orientations are measured from the north; negative signs indicate that they are measured in the counter-clockwise direction.

(a) No Leaves

Date & hour	U_H[m s^{-1}]	LAI	Bearing	Stability H/L
3/11 13–15	1.72	0	W(–127° ≤ θ ≤ –101°)	– 0.288
3/19 13–15	2.45	0	SW(–130° ≤ θ ≤ –104°)	– 0.031
3/23 6–8	1.83	0	SW(–150° ≤ θ ≤ –129°)	0.243

(b) With leaves

Date & hour	U_H[m/s]	LAI	Bearing	Stability H/L
11/14 16–18	1.72	1.49	SW(–144° ≤ θ ≤ –126°)	0.723
11/16 13–15	1.95	1.49	SW(–138° ≤ θ ≤ –116°)	– 0.168
11/27 12–14	1.97	1.49	SW(–138° ≤ θ ≤ –127°)	– 0.094

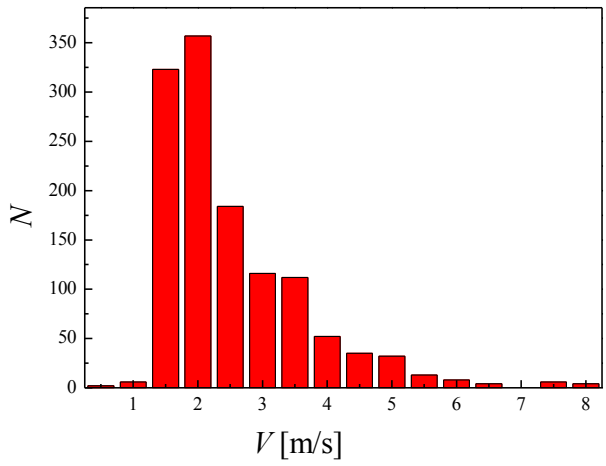

Figure 4(a)

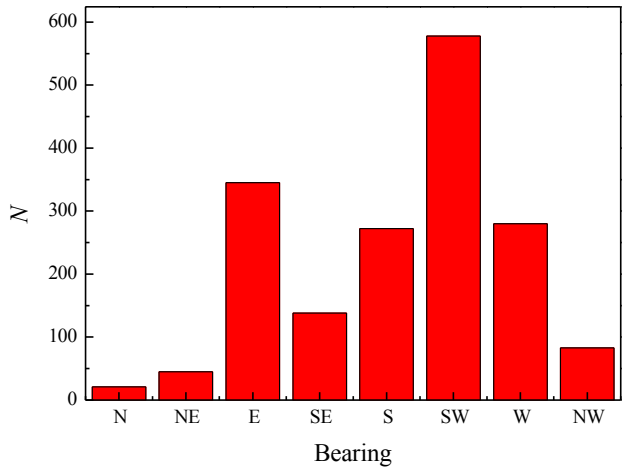

Figure 4(b)

Figure 4. Probability densities of two-hour averaged values of (a) wind velocity and (b) wind bearing over a period of five months, from early November 2009 to the end of March 2010.

3 Vertical Profiles of Time-Averaged Horizontal Mean Wind

Vertical profiles of mean horizontal wind velocity in the open space above a vegetation canopy have been already reported by many authors during the last few decades. It was found that the profiles obey the well-known logarithmic law [e.g. Kaimal & Finnigan (1994)],

$$\overline{U}(z) = \frac{u_*}{\kappa} \ln \frac{z-d}{z_0}, \tag{1}$$

where u_* is the friction velocity, z_0 is the roughness length, d is the zero-plane displacement height, and κ is the von Karman constant. On the other hand, vertical profiles of mean velocity within a vegetation canopy were derived by Inoue (1963) and Cionco (1965) independently, assuming a constant mixing length within the canopy:

$$\overline{U}(z) = \overline{U}_{\mathrm{H}} \exp\left[-b\left(1-\frac{z}{H}\right)\right]. \tag{2}$$

Here $\overline{U}_{\mathrm{H}}$ is the mean horizontal wind speed at the top of the canopy and b is the attenuation constant, reflecting the canopy density. Firstly, we are interested in which profile can better describe the vertical profiles of $\overline{U}(z)$ in the canopy, particularly when the deciduous trees have completely lost their leaves. Hence, we plotted the normalized mean wind speed $\overline{U}(z)/\overline{U}_{\mathrm{H}}$ against the normalized height z/H.

As is seen from Figure 5(a), even though the trees have no leaves, the exponential profile is a good fit. Probably bare branches and twigs still provide sufficient aerodynamic resistance, so that the constant-mixing-length hypothesis is marginally valid. When the trees have some leaves, the exponential profile is the better candidate to describe the velocity profile, as shown in Figure 5(b). From these observations, we conclude that normalized vertical profiles of mean velocity $\overline{U}(z)/\overline{U}_{\mathrm{H}}$ obey an exponential law regardless of amount of leaves in the deciduous forest canopy, provided the stem density is sufficiently large (as in the present case).

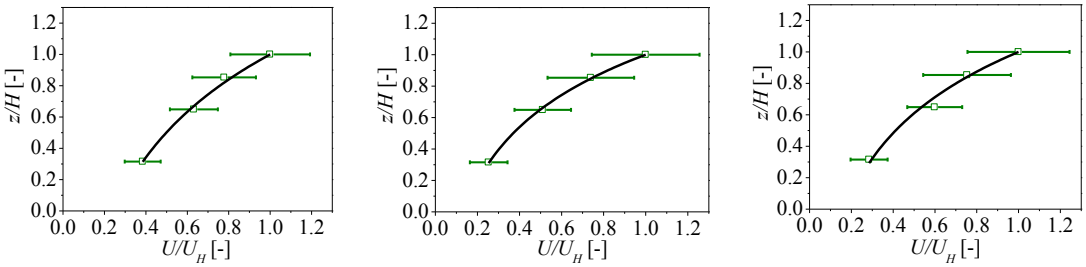

March 11
13–15 hour

March 19
13–15 hour

March 23
6–8 hour

(a) No leaves

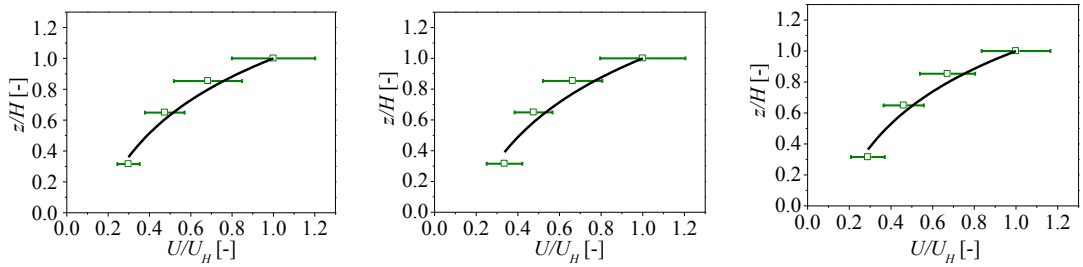

Nov. 14
13–15 hour

Nov. 19
13–15 hour

Nov. 23
12–14 hour

(b) With leaves

Figure 5. Vertical velocity profiles of horizontal wind velocity:
(a) trees with no leaves, early spring in 2010; (b) trees with leaves, late autumn in 2009.

4 Eddy Diffusivities

4.1 Mixing Length based on von Karman's Geometrical Similarity

The mixing length is an important parameter to describe the mechanisms underlying turbulent-transport processes; the turbulent diffusion coefficient can be defined as a product of the mixing length and the root-mean-square value of the fluctuating components, i.e. the intensity of turbulence. In the present study, we calculated the values of mixing length using Equation (3) below, which is based on the law of Karman's assumption of geometrical similarity [e.g. Schlichting (1968), Hinze (1975)]:

$$l = \kappa \left| \frac{d\bar{U}/dz}{d^2\bar{U}/dz^2} \right| \tag{3}$$

The mixing length is given by the ratio of two consecutive derivatives, e.g. the first and the second derivatives, of the mean velocity profile. In particular, if we assume the exponential law, the mixing length l takes a constant value within the entire forest canopy. The calculated mixing lengths on respective days are shown in Table 2. The average value of l is about $0.24H$ when the trees have no leaves. On the other hand, it is about $0.21H$ when the trees have some leaves (50% of the full foliage). The difference is not great, and this indicates that bare branches and twigs still produce a significant aerodynamic resistance.

Table 2. Eddy diffusivities at z = 22.5 m based on the length scale obtained from the von Karman method. Each one is an averaged value over a period of two hours.

(a) No leaves

Date & hour	b	Mixing length l [m]	K_U [m^2/s]	K_W [m^2/s]
3/11, 13–15	1.4	6.63	6.88	3.84
3/19, 13–15	1.99	4.59	5.06	3.05
3/23, 6–8	1.78	5.20	3.82	1.64

(b) Leaves

Date & hour	b	Mixing Length l [m]	K_U [m^2/s]	K_W [m^2/s]
11/14, 16–18	1.89	4.88	5.88	4.04
11/16, 13–15	1.79	5.16	5.78	4.21
11/27, 12–14	1.95	4.74	5.56	3.96

4.2 Length scales deduced from autocorrelation of $u(t)$ and friction velocity u_*

Another statistical property of time-dependent fluctuating components is the autocovariance of the variable in time. It is the measure of the relationship between values of $u(t)$ at two different times.

$$T = \int_0^\infty \rho(\tau)d\tau, \quad \text{where} \quad \rho(\tau) = \overline{u(t)u(t+\tau)} \Big/ \overline{u^2(t)} \tag{4}$$

The integral in Equation (4) yields a time scale for $u(t)$. The above-defined time scale can be viewed as the time interval over which the random $u(t)$ remains correlated with itself, i.e. a turn-over time scale of turbulent eddies. This time scale may be multiplied by the mean wind velocity, defining another length scale which characterizes the length scale in the mean wind direction:

$$l_U = T\overline{U} \ . \tag{5}$$

The length scales thus obtained are listed in Table 3, together with the eddy diffusion coefficients computed by multiplying with the turbulent intensities, as seen in the following section. It should be noted that l_U is now dependent on z.

The vertical length scale, on the other hand, may be taken from the commonly-used friction velocity, which relates the vertical momentum transfer and the vertical velocity gradients:

$$l_W = \frac{u_*}{d\overline{U}/dz} = \frac{\sqrt{-\overline{u'w'}}}{d\overline{U}/dz} = \frac{\sqrt{-\overline{u'w'}}}{\overline{U}_H \dfrac{b}{H} \exp\left[-b\left(1-\dfrac{z}{H}\right)\right]} \ . \tag{6}$$

It is clear that l_W is also a function of the height z.

It should be mentioned that defining the length scales as in Equations (5) and (6) are contradictory, in the strict sense, to the original assumption that the vertical velocity profiles in the canopy are exponential, since Equation (2) is the theoretical consequence of the constant mixing length in the forest canopy. Therefore, formally, we have to take the exponential profile as a mere empirical relation when we make use of Equations (5) and (6).

4.3 Eddy Diffusion Coefficient

We express each component of the eddy diffusion coefficient in the x, y, and z directions as described below:

$$K_U = l\sqrt{\overline{u'^2}},\ K_V = l\sqrt{\overline{v'^2}},\ K_W = l\sqrt{\overline{w'^2}}\ , \tag{7}$$

where u' , v' , and w' are the fluctuations of the respective wind velocity components, u, v, and w, while l is the mixing length calculated using Equation (3). The eddy diffusion coefficient K is equal to the product of the mixing length and the root-mean-square of velocity fluctuations (the turbulent intensities). This is the expression derived by Prandtl from the analogy between kinetic theory of gases and turbulent eddy motion, in which he hypothesizes that the kinematic viscosity is equal to the product of the turbulent intensity and the Lagrangian length scale [e.g. Fischer *et al*. (1979)]. The results evaluated at the elevation z = 22.5 m are summarized in Table 2. The diffusivities K_U , about 5 $m^2\ s^{-1}$, are nearly independent of the LAI, and they decrease with descent into the canopy, due to the decaying turbulent intensities (see also Figures 9 and 10). The anisotropy between the values in the horizontal (principal) direction and the vertical direction is not great, but still visible, while the vertical diffusivities are approximately 50% of the horizontal values. It may be noticed that the anisotropy is reduced when the canopy has leaves.

Figure 6 shows how the eddy diffusion coefficient K depends on the horizontal wind speed. Figure 6(a) shows the horizontal diffusivities, while Figure 6(b) shows the vertical diffusivities, both as a function of horizontal wind speed. Each plot presents 10-minute average values, taken from the six different days, as well as a few other windy days with similar atmospheric conditions in stability and wind bearing. At first appearance, the wide scattering of the data in March, compared with those in November, is evident, which might suggest that the source of the turbulent eddies seen within the canopy in March is not necessarily the canopy itself, but the surrounding topography. When the trees have leaves, the canopy's outer-layer property is hindered by the turbulent generation due to canopy itself. Consequently the differences between the horizontal and vertical components of K are less visible, and the horizontal diffusivities are only about 1.5 times larger than the vertical values. In contrast, when the trees have no leaves, the horizontal components K_U are about twice those of the vertical components K_W. It appears that the anisotropy of K depends on the amount of leaves in the forest canopy, and that the leaves generally reduce the anisotropy between the two components. The finding is consistent with Table 2. This seems quite natural if one imagines that the leaves are likely to enhance random turbulent wakes within the forest canopy.

The von Karman method produces only one length scale, l , independent of the height z and the coordinate directions. Equation (7), on the other hand, generates three different components of anisotropic diffusivity based on a single length scale. It seems more natural, however, to think that each component has an associated inherent length scale, different from each other. Therefore we may alternatively use the horizontal length scale based on the integral time scale of $u(t)$, given by Equation (5), and the vertical one by Equation (6). Multiplication by the respective turbulent intensities allows the horizontal and vertical eddy diffusivities to be obtained. The results from 14 November, 2009 and 11 March, 2010 at four different heights are summarized in Table 3. It can be immediately seen that for the upper region of the 11 March data, values are four to ten times larger than those obtained by the previous method, while for the other cases the results based on the integral time scale are more or less consistent with Table 2 and Figure 6.

It is plausible that the open atmosphere (the canopy's outer layer) is readily filled with large-scale turbulent eddies, generated by the non-uniform topography. These eddies can penetrate down into the canopy sub-layer when it does not have leaves and the canopy is sparse. In fact the length scale of 50 m is consistent with the ridge widths in the surrounding area. While the canopy has leaves, the boundary between the canopy and the open atmosphere, with a sharp change in aerodynamic resistance, can generate turbulent eddies due to Kelvin-Helmholtz shear instability, with a scale that is independent of the open-air conditions. The scale will be of order at most the canopy height, bounded by the presence of the ground. This commonly-accepted mechanism of turbulence generation in the canopy may be dominant when the canopy has leaves, and be responsible for the smaller length scales deduced from the analysis above.

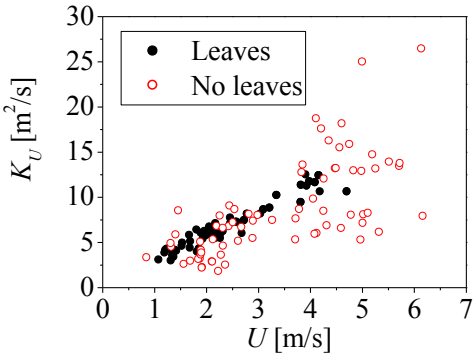

(a)

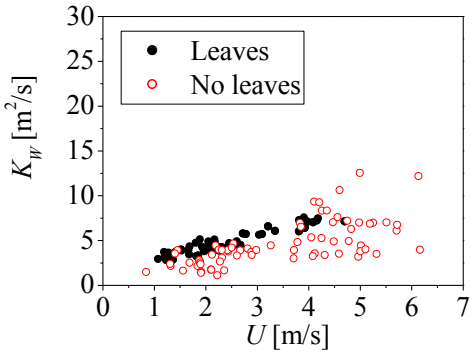

(b)

Figure 6. Horizontal and vertical eddy diffusivities as a function of wind speed based on von Karman's method: (a) horizontal eddy diffusivities K_U; (b) vertical eddy diffusivities K_W. Each plot point represents a value averaged over ten minutes. The data include values at different heights. We also added data obtained on more windy days, keeping the other conditions (atmospheric stability and wind bearings) the same as those in Figure 4.

Table 3. Eddy diffusivities at four different heights based on the length scale obtained from the integral time scale and friction velocity. Each one is an averaged value over a period of two hours.

Table 3 (a) No leaves (13–15 hour, 11 March, 2010)

Height [m]	Integral Time Scale T [s]	Horizontal Length Scale l_U [m]	Vertical Length Scale l_W [m]	K_U [m^2 / s]	K_W [m^2 / s]
22.5	29.5	65.9	2.70	76.1	3.22
19.2	29.4	21.8	3.53	19.6	2.18
14.6	28.3	14.5	3.49	10.2	1.58
7.1	25.3	6.28	4.84	3.2	1.68

Table 3 (b) With leaves (16–18 hour, 14 November, 2009)

Height [m]	Integral Time Scale T [s]	Horizontal Length Scale l_U [m]	Vertical Length Scale l_W [m]	K_U [m^2 / s]	K_W [m^2 / s]
22.5	6.05	10.4	2.43	10.7	1.87
19.2	5.34	3.95	3.43	3.60	2.19
14.6	5.28	2.70	2.31	1.35	0.931
7.1	6.71	1.67	3.89	0.632	0.864

5 Turbulent Eddy Structures

5.1 Quadrant Analysis

Quadrant analysis is one of the methods for identifying the turbulent structures. Each fluctuating component u' and w' is plotted on two-dimensional Cartesian coordinates from the data generated with a 1 Hz sampling rate. The plots falling in the second quadrant ($u' < 0,\ w' > 0$) can be identified as "ejection", while those in the fourth quadrant ($u' > 0,\ w' < 0$) are termed "sweep". The sweep and ejection are characterized by the motion of high-velocity fluid parcels from the upper layer moving downward into the forest canopy, followed by relatively low-velocity fluid parcels from the canopy sub-layer moving upward to the open air. Air motion in the remaining two quadrants can be identified as "interaction" between ejection and sweep [e.g. Wallace *et al*. (1972)]. The second and the fourth quadrants, representing ejections and sweeps, are the primary source of generating turbulent energy.

Figures 7 and 8 show the results of quadrant analysis. The graphs in Figure 7 present the data from 11 March, 2010 and those in Figure 8 are from the data on 14 November, 2009. As shown in Figure 7, when the trees have no leaves, it is found that correlations between u' and w' have more or less negative slopes and that they decay with the depth in the forest. In addition, the sweep motions appear stronger than those of ejection. On the other hand, as shown in Figure 8, when the canopy has some leaves, the correlations between u' and w' are less visible, although they still have negative slopes. This is probably due to the more random wake motions produced by the presence of leaves and their waving motions. This is consistent with our previous observation about the turbulent diffusivities: that the leaves make the turbulent diffusivities more isotropic.

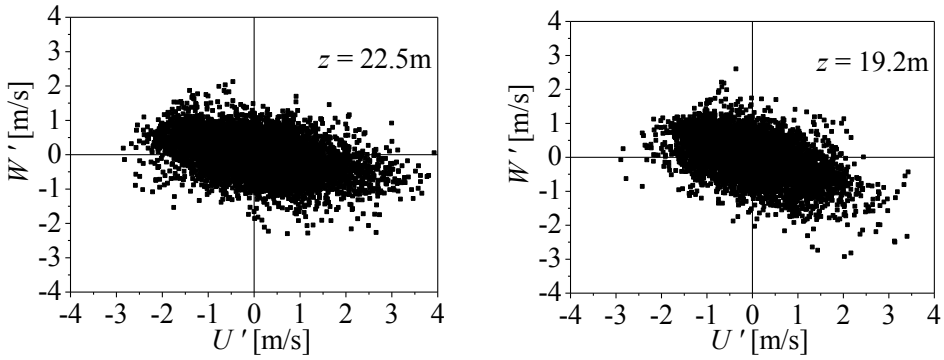

Figure 7 (part): see below for description.

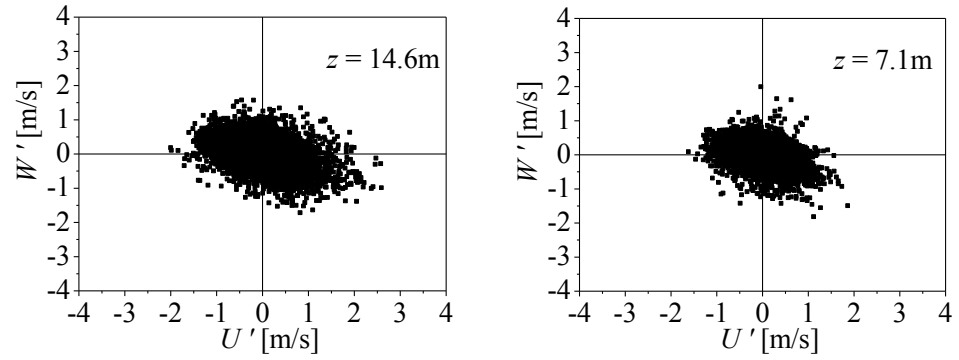

Figure 7. Quadrant analysis for horizontal and vertical fluctuating components at different heights, when trees have no leaves: 13:00–15:00, 11 March, 2010. The sampling rate is 1 Hz, and 7200 points are plotted.

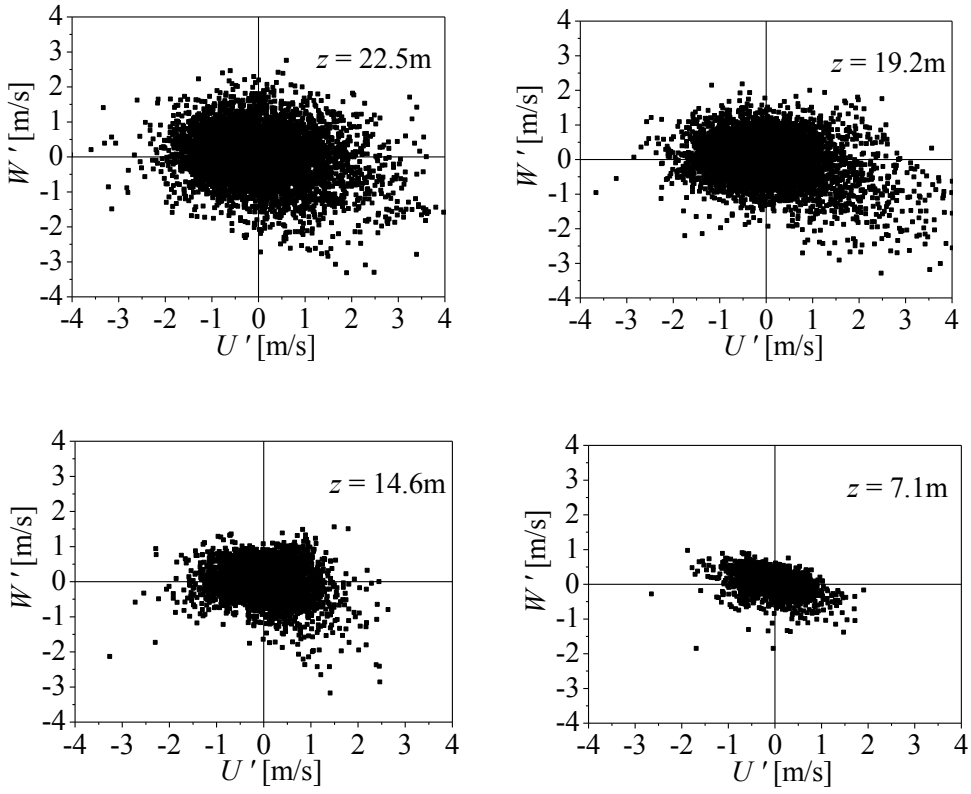

Figure 8. Quadrant analysis for horizontal and vertical fluctuating components at different heights, when trees still have leaves: 13:00–15:00, 14 November, 2009. The sampling rate is 1 Hz, and 7200 points are plotted.

5.2 Spectral analysis of u' and w'

Figures 9 and 10 show a few examples of time series correlations of u' and w' at four different heights. The graphs in Figure 9 are based on the measurements on 11 March, 2010, while those in Figure 10 are based on the measurements on 14 November, 2009. For the case of no leaves (Figure 9), it can be clearly seen that the

products $u'w'$ at four different heights in the forest canopy are mostly negative. This observation is consistent with our quadrant analysis as seen in Figure 7. It seems that "sweep and ejection" is active throughout the canopy sub-layer. On the other hand, when the canopy has leaves, the products of $u'w'$ do not show any clear negative signs in the time-series of u' and w' in Figure 10. It can be also seen that the frequencies of u' and w' observed in Figure 10 are higher than those in Figure 9. This observation is further reinforced by using spectral analysis, as seen in Figure 11. In Figure 11(b) the spectra in the higher frequency range are more pronounced, compared with those in Figure 11(a). Again, a possible implication is that the presence of leaves generates a finer eddy structure by waving motions in the forest canopy. However, in neither case is a dominant frequency found.

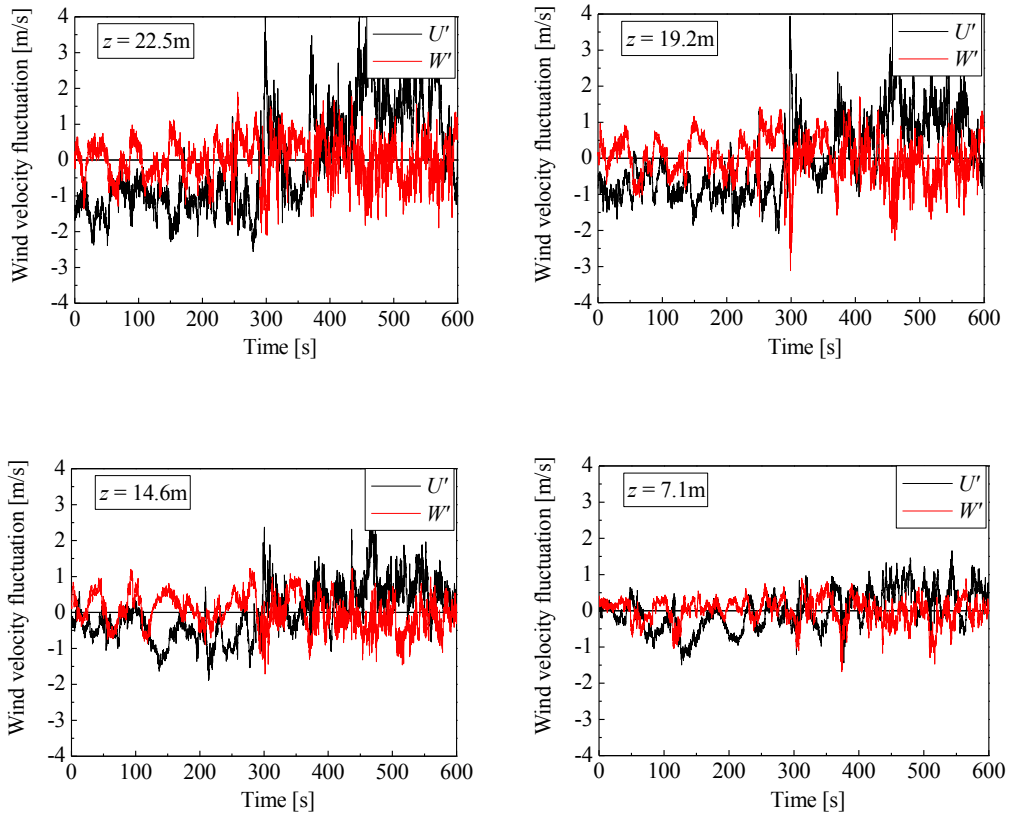

Figure 9. Time series of fluctuating components u' and w': 13:00–13:10, 11 March 2010.

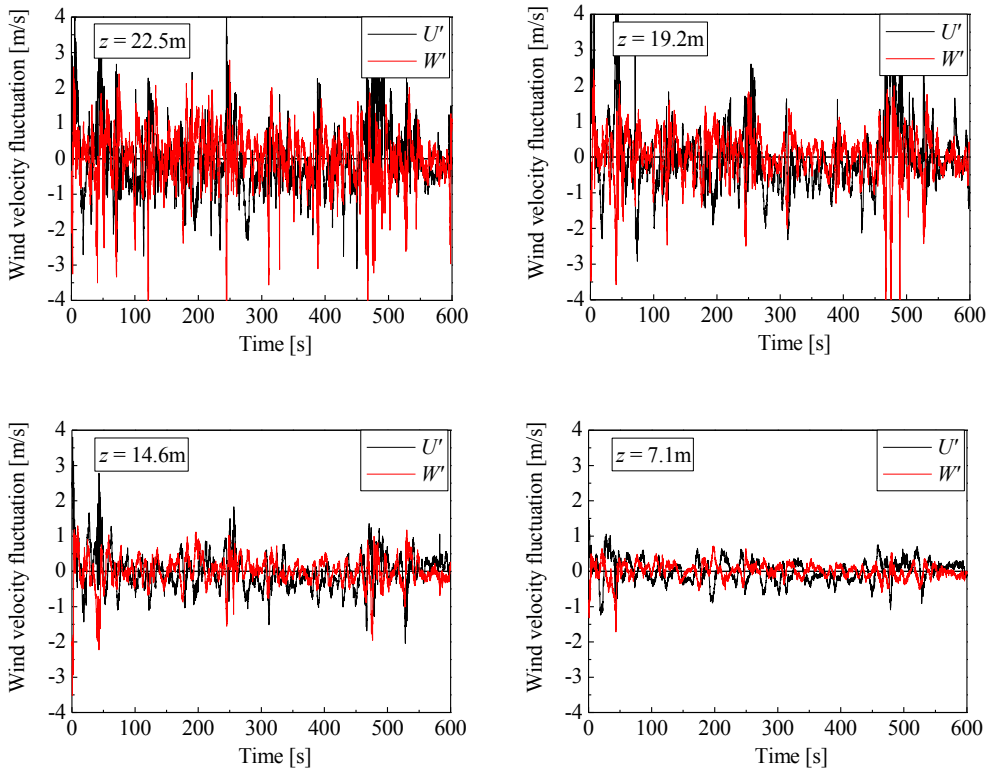

Figure 10. Time series of fluctuating components u' and w': 13:00-13:10, 14 November 2010.

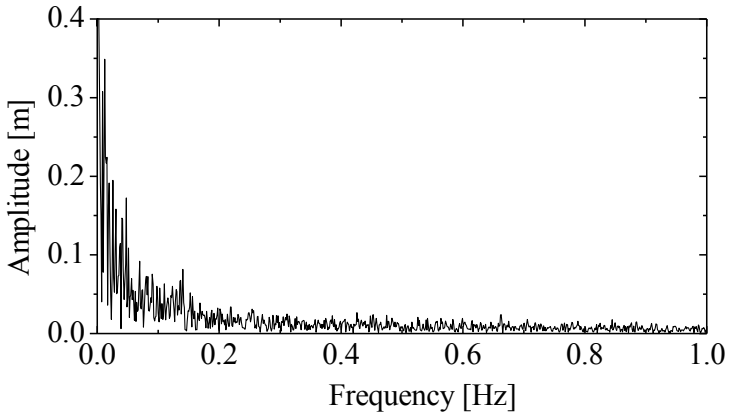

Figure 11(a)

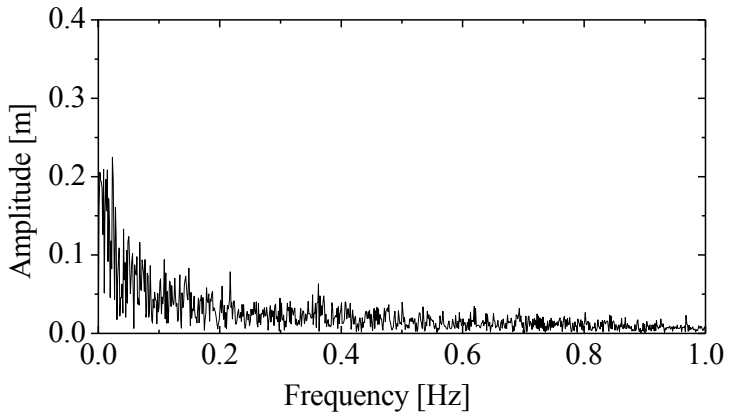

Figure 11(b)

Figure 11. Spectral analysis of time series of fluctuating component u' : (a) 11 March, 2010; (b) 14 November, 2009. Data sampled at 10 Hz over a period of ten minutes were used for the spectral analysis.

6 On the Effects of Surrounding Topography

In our previous analyses, we neglected the effects of topography, and assumed that the time-averaged z-components of wind velocity are always zero, i.e. the time-averaged wind is horizontal. However, the data analysis reveals that the average z-components are not necessarily zero, but have measurably finite values. The formally-reported results above ignored the mean vertical component of the wind. Figure 12 shows the total mean wind-speed $\bar{U}_0 = \sqrt{\bar{u}^2 + \bar{v}^2 + \bar{w}^2}$ (continuous lines) and the horizontal mean wind-speed $\bar{U} = \sqrt{\bar{u}^2 + \bar{v}^2}$ (dashed lines) over a period of two hours, at the four different heights. Because the wind seems to be not far from horizontal near the canopy top (at z = 22.5 m, 19.2 m), the two lines are very close. However, further down in the canopy, the surface topography appears to have a strong effect (also see Figure 13), and the wind-speed values differ more. Figure 13 shows α, the angle of the wind from the horizontal at each level, averaged over the 10-minute periods. Here, $\tan a = \bar{w} / \sqrt{\bar{u}^2 + \bar{v}^2} = \bar{w} / \bar{U}$. The values of α are all negative, probably reflecting the steep descending slope to the east of the tower (see Figure 1). Both figures show that there is a marked vertical component of mean wind-speed in the lower part of the canopy. The wind angle is up to 35° below the horizontal in the lower part of the canopy. Also, the wind direction changes by up to 25° from top to bottom, as shown in Figure 13. The attenuation coefficient b in the formula (2) for both cases are shown in Figure 14 where, first, the vertical wind component is ignored and the values are based on the horizontal wind only (b, dashed line), and also where the total wind-speed is included in the calculations (b_0, continuous line). The means of the 12 values calculated from the 10-minute periods are b = 1.290 and b_0 = 1.141 respectively. The relative difference is 11.6% in this particular two-hour data set of 14 November, 2009. The associated effects on the eddy diffusivities are expected to be of the same order of magnitude.

Figure 15 shows three-dimensional wind velocities at four different heights. Figure 15(a) with no leaves is drawn using the ten-minute average data in the morning of 23 March, 2010, and Figure 15(b) with leaves is based on those data in the afternoon of 14 November, 2009. It is interesting to note that, as the measurement position is lowered, the wind bearing shifts towards the south. The trend is consistent in the both cases. Since the ground level dives towards the east at about 30°, and descends gradually towards the north as well at about 16°, it appears that the lower wind is apt to blow parallel to the ground slopes.

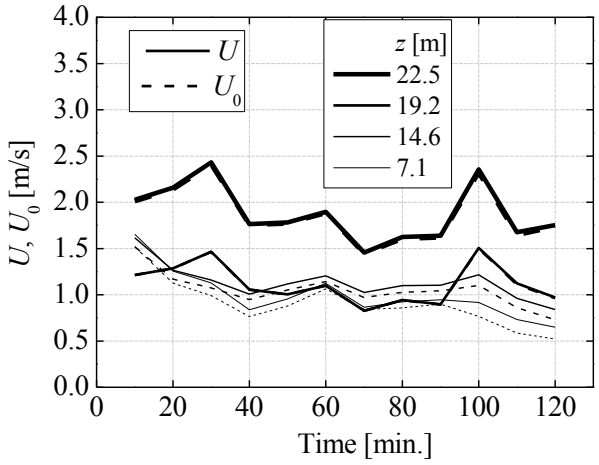

Figure 12. The total mean wind-speed $\overline{U}_0 = \sqrt{\overline{u}^2 + \overline{v}^2 + \overline{w}^2}$ (continuous lines) and the horizontal mean wind-speed $\overline{U} = \sqrt{\overline{u}^2 + \overline{v}^2}$ (dashed lines) at four different levels. The plots are made from the data of 13:00-15:00, 14 November, 2009.

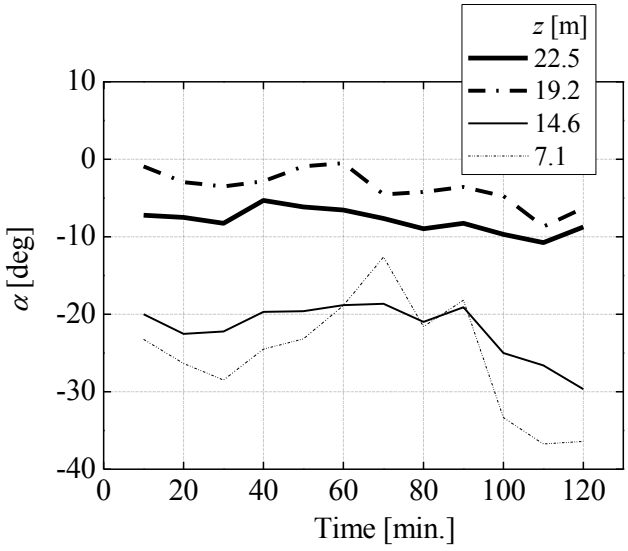

Figure 13. The diving angles α, in degrees, of the direction of the wind from the horizontal plane at each level, averaged over the 10-minute periods. The plots are made from the data acquired in the same period of time as in Figure 11.

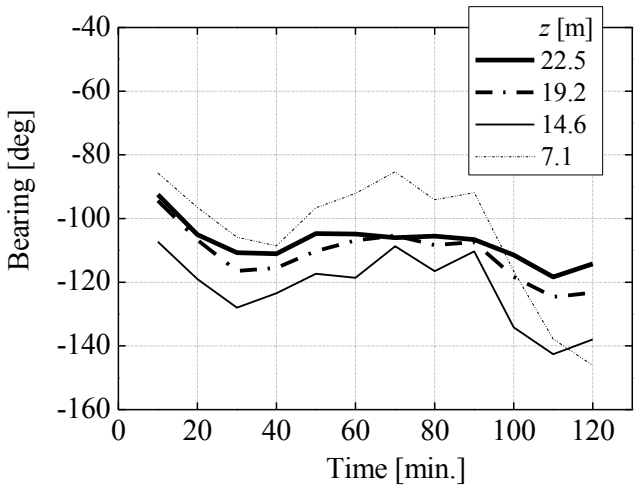

Figure 14. The bearings of the wind at four different levels in the two-hour period 13:00–15:00, 14 Nov., 2009.

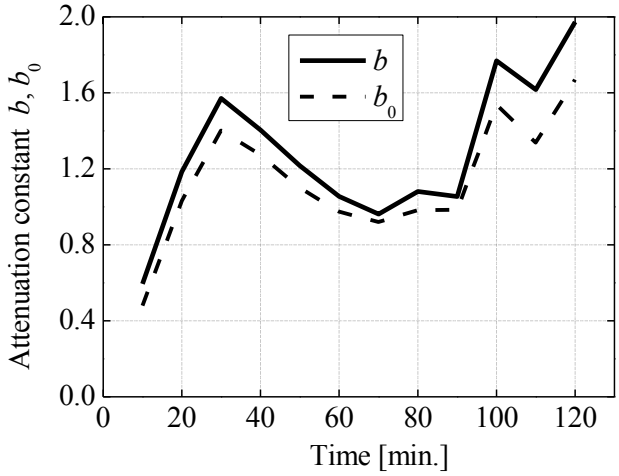

Figure 15. The time-variation of the attenuation coefficients b computed from Equation (2) based on the data 13:00-15:00, 14 November, 2009. The values of b_0 are computed using the total wind speed profiles over the same period of time.

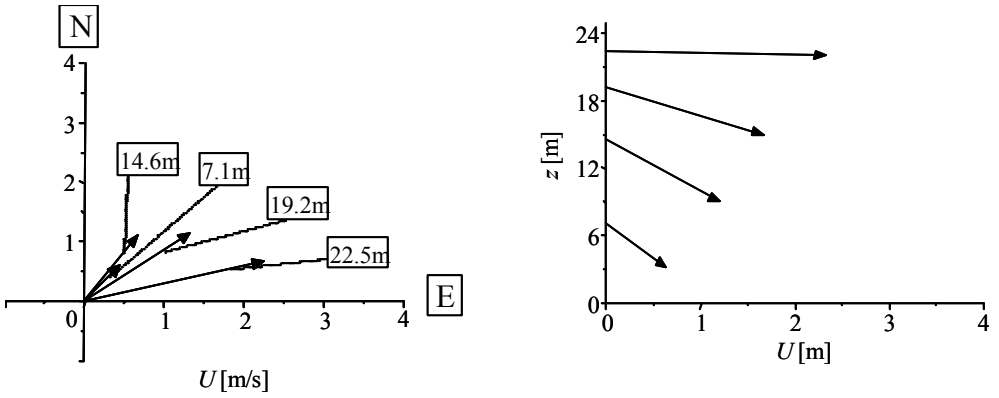

(a)

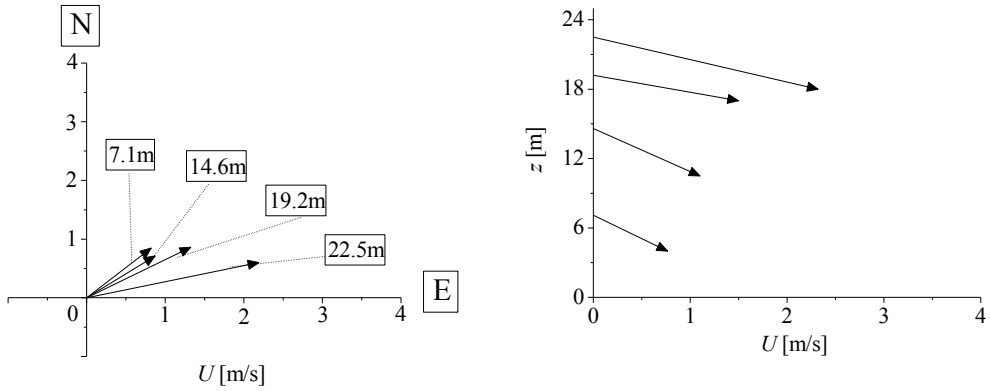

(b)

Figure 16. Three-dimensional wind velocity vectors at four different heights: (a) average values over 7:50-8:00, 23 March, 2010; (b) average values over 13:30-13:40, 14 November, 2009.

7 Conclusions

We have carried out field measurements of wind velocities in an oak forest covering a complex topographical terrain, using four 3-D sonic anemometer-thermometers mounted on the 20 m tall observation tower, during a period of five months from November of 2009 to March of the next year. We picked two sets of data, each of which consists of observations over two hours on different days, but all of them are similar in mean wind velocity, wind bearing and atmospheric stability, in order to delineate the effect of LAI on the turbulent diffusivities. The following conclusions are made:

(1) Normalized vertical profiles of the mean velocity $\overline{U}(z)/\overline{U}_{\mathrm{H}}$ can be approximated with an exponential function regardless of leaf density in the forest canopy.

(2) Based on von Karman's method and exponential velocity profiles, computed mixing lengths l_{H} are equal to about $0.21H$ when the trees have leaves in November, while they are slightly greater or equal to $0.24H$ when the trees have no leaves in March.

(3) The length scales based on autocorrelations of wind velocity fluctuations are also computed. The results are more or less consistent with von Karman's method with exponential profiles, when the trees have leaves. The length scales are about 5-6 m, which is about 25% of the canopy height. However, when the trees have no leaves, significantly different values in the upper region in the canopy sub-layer are found in the mean wind direction, where the obtained length scales are order of 50 m, a characteristic length in the surrounding topography.

(4) The eddy diffusion coefficients K depend on both the wind velocity and the leaf density. They generally take larger values when the mean wind velocity is large. The anisotropy of K is pronounced when no leaves are present, and the values in the mean wind direction are two to ten times greater than the vertical ones. The anisotropy tends to diminish when the tree leaves are dense.

(5) Using a quadrant analysis, it is found that, when the canopy has no leaves, the products $u'w'$ tend to take negative values, and a pair of ejection and sweep events are more evident at the top and within the canopy layer. However, it is less obvious when the canopy has leaves.

(6) Comparing the time series of two different fluctuating components u' and w', it is found that the fluctuating frequencies take higher values when the canopy has leaves than those when it has no leaves. This is probably due to more active waving motions of branches and twigs when trees have leaves.

(7) Some effects of surrounding topography are found in both the mean wind angle from the horizontal and the wind bearing. It appears that the effects are more visible in the lower layer in the canopy. The effects of these mean wind variations on the turbulent diffusivities are estimated to be order of 10%. However, when the canopy does not have leaves, the turbulent eddies in the outer-layer can penetrate into the upper region of the canopy sub-layer, resulting in a one-order larger diffusivity in the mean wind direction.

Acknowledgements

We gratefully acknowledge technical supports provided by Mr Tomohiro Kuratani, technician, and Mr Yusuke Itoh, graduate student, from the School of Mechanical Engineering, Kanazawa University.

References

Allen, L.H. Jr, Turbulence and wind speed spectra within a Japanese larch plantation, *J Appl Meteorol*, **7**:73-78, 1968.

Amiro, B.D., Drag coefficients and turbulence spectra within three boreal forest canopies, *Boundary-Layer Meteorol*, **52**:227-247, 1990.

Cionco, R.M., A mathematical model for air flow in a vegetation canopy, *J App Meteorol*, **43**:345-346, 1965.

Finnigan, J.J., Turbulence in waving wheat. 2: Structure of momentum transfer, *Boundary-Layer Meteorol,* **16**:213-236, 1979.

Finnigan, J.J., Turbulence in plant canopies, *Ann Rev Fluid Mech*, **32**:519-571, 2000.

Fischer, H.G., List, E.G., Koh, R.C.Y., Imberger, J. and Brooks, N.H., *Mixing in inland and coastal waters*. Academic Press, New York, 483pp, 1979.

Gao, W., Shaw, R.H. and Paw U, K.T., Observation of organized structure in turbulent flow within and above a forest canopy, *Boundary-Layer Meteorol*, **47**:349-377, 1989.

Harper, S.A., McKibbin, R. and Wake, G.C., An advection-dispersion model for spray droplet transport including interception by a shelterbelt, In: Fitt, A.D., Norbury, J., Ockendon, H. and Wilson, E. (eds), *Progress in Industrial Mathematics at ECMI 2008*, Series: Mathematics in Industry, Subseries: The European Consortium for Mathematics in Industry, Vol. 15, 1st Edition. Springer-Verlag, Berlin, Heidelberg, 1050 p, 2010. ISBN: 978-3-642-12109-8. <doi:10.1007/978-3-642-12110-4_139>

Hinze, J.O., *Turbulence*, 2nd edition. McGraw Hill, 1975.

Inoue, E., Studies on the phenomena of waving plants ("Honami") caused by wind. I. Mechanism and characteristics of waving plants phenomena, *J Agric Meteorol Tokyo*, **11**:87-90, 1955.

Inoue, E., On the turbulent structure of the airflow within crop canopies, *J Meteorol Soc Japan*, **41**:317-326, 1963.

Kaimal, J.C. and Finnigan, J.J., *Atmospheric boundary-layer flows*. Oxford University Press, 1994.

Kantha, L.H. and Clayson, C.A., *Small-scale processes in geophysical flows*. Academic Press, New York, 888pp, 2000.

Kondo, J. and Akashi, S., Numerical studies of the two-dimensional flow in horizontally homogeneous canopy layers, *Boundary-Layer Meteorol*, **10**:255-272, 1975.

Langre, E., Effects of wind on plants, *Ann Rev Fluid Mech*, **40**:141-168, 2008.

Launiainen, S., Vesala, T., Mölder, M., Mammarella, I., Smolander, S, Rannik, Ü., Kolari, P., Hari, P., Lindroth, A. and Katul, G.G., Vertical variability and effect of stability on turbulence characteristics down to the floor of a pine forest, *Tellus*, **59B**:919-936, 2007.

Lim, L.L., Sweatman, W.L., McKibbin, R. and Connor, C.B., Tephra fallout models: The effect of different source shapes on isomass maps, *Mathematical Geosciences*, **40**:147-157, 2008. <doi:10.1007/s11004-007-9134-4>

Lim, L.L., Sweatman, W.L. and McKibbin, R., A simple deterministic model for volcanic ashfall deposition, *The ANZIAM Journal*, **49**(3): 325-336, 2008. <doi:10.1017/S1446181108000047>

Marcolla, B., Pitacco, A. and Cescatti, A., Canopy architecture and turbulent structure in a coniferous forest, *Boundary-Layer Meteorol*, **108**:39-59, 2003.

McKibbin, R., Discovering the source of current-borne particles from their deposition pattern, *Proc. International Symposium of the Kanazawa University 21st-century COE Program – Environmental Monitoring and Prediction of Long- and Short-Term Dynamics of Pan-Japan Sea Area: Construction of Monitoring Network and Assessment of Human Effects*, Kanazawa University, Japan, 191-196, 2003.

McKibbin, R., Lim, L.L., Smith, T.A. and Sweatman, W.L., A model for dispersal of eruption ejecta, *Proceedings of the World Geothermal Conference 2005, Antalya, Turkey, 24-29, April, 2005,* International Geothermal Association, Paper no. 0715. ISBN 975-98332-0-4 (CD).

McKibbin, R., Modelling pollen distribution by wind through a forest canopy, *JSME International Journal, Series B* **49**(3):583-589, 2006.

McKibbin, R., Mathematical modelling of aerosol transport and deposition: Analytic formulae for fast computation, *Proceedings of the iEMSs Fourth Biennial Meeting, International Congress on Environmental Modelling and Software (iEMSs 2008)*, *Barcelona, Spain, 7 – 10 July 2008,* iEMSs, 1420-1430, 2008.

McKibbin, R., Mathematical modeling of aerosol transport: effect of dispersion coefficients on predicted ground deposits, *21st International Symposium on Transport Phenomena, Kaohsiung City, Taiwan, 2-5 November 2010*, National Kaohsiung University of Applied Sciences, Taiwan , 1372-1380, 2010. ISBN 978-986-6184-23-3 (CD)

Oikawa, S. and Meng, Y., Turbulence characteristics and organized motion in an urban roughness sublayer, *Boundary-Layer Meteorol* , **74**:289-312, 1995.

Poggi, D., Porporato, A., Ridolfi, L., Albertson, J.D. and Katul, G.G., The effect of vegetation density on canopy sub-layer turbulence, *Boundary-Layer Meteorol*, **111**:565-587, 2004.

Raupach, M.R. and Thom, A., Turbulence in and above plant canopies, *Ann Rev Fluid Mech*, **13**:97-129, 1981.

Raupach, M.R., Finnigan, J.J. and Brunet, Y., Coherent eddies and turbulence on vegetation canopies: the mixing layer analogy, *Boundary-Layer Meteorol*, **78**:351-382, 1996.

Rotach, M.W., Turbulence close to a rough urban surface. Part 1: Reynolds stress, *Boundary-Layer Meteorol*, **65**:1-28, 1993.

Roth, M. and Oke, T.R., Turbulent transfer relationships over an urban surface: Spectral characteristics, *Quart J Royal Meteorol Soc* , **119**:1071-1104, 1993.

Schleppi, P., Conedera, M., Sedivy, I. and Thimonier, A., Correcting non-linearity and slope effects in the estimation of the leaf area index of forests from hemispherical photographs, *Agricultural and Forest Meteorol*, **144**:236-242, 2007.

Schlichting, H., *Boundary-Layer Theory*, 6th edition. McGraw Hill, 1968.

Shaw, R.H., Den Hartog, G., King, K.M. and Thurtell, G.W., Measurements of mean wind flow and three-dimensional turbulence intensity within a mature corn canopy, *J Agric Meteorol*, **13**:419-425, 1974.

Uchijima, Z., Studies on the microclimate within plant communities, *J Agric Meteorol*, **18**:1-10, 1962.

Uno, I., Wakamatu, S.H. and Nakamura, A., An observation study of the structure of the nocturnal urban boundary layer, *Boundary-Layer Meteorol*, **45**:59-82, 1988.

Wallace, J.M., Eckelmann, H. and Brodkey, R.S., The wall region in turbulent shear flow, *J Fluid Mech*, **54**:39-48, 1972.

Yi, C., Moment transfer within canopy, *J Appl Meteorol and Climatology*, **47**:262-275, 2008.